Science of the Total Environment 774 (2021) 145170

Contents lists available at ScienceDirect

Science of the Total Environment

journal homepage: www.elsevier.com/locate/scitotenv

Insights into the degradation and toxicity difference mechanism of neonicotinoid pesticides in honeybees by mass spectrometry imaging

Yue Zhang [a,c,1], Dong Chen [a,1], Mingyi Du [a], Lianlian Ma [a], Ping Li [a], Run Qin [a,c], Jiaru Yang [a], Zhibin Yin [b,*], Xinzhou Wu [a,*], Hanhong Xu [a,*]

[a] State Key Laboratory for Conservation and Utilization of Subtropical Agro-bioresources and Key Laboratory of Natural Pesticide and Chemical Biology of the Ministry of Education, South China Agricultural University, Guangzhou 510642, China
[b] Agro-biological Gene Research Center, Guangdong Academy of Agricultural Sciences, Guangzhou 510640, China
[c] Key Laboratory of Bio-Pesticide Creation and Application, Guangzhou 510642, China

HIGHLIGHTS

- Dinotefuran and acetamiprid can quickly penetrate through biological barriers of honeybees.
- Toxicity difference of neonicotinoids to honeybees lies in distinct degradation rate.
- Degradation rate of acetamiprid is decreased with PBO applied, but not for dinotefuran.
- Tebuconazole slows down the degradation of acetamiprid due to synergistic effect.
- Difference degradation of neonicotinoids in honeybees is related to CYP450 superfamily.

GRAPHICAL ABSTRACT

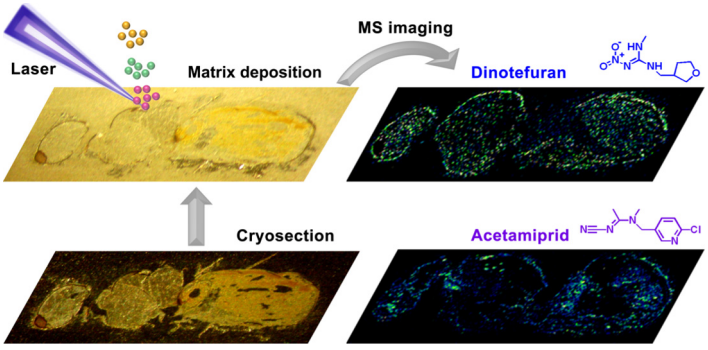

ARTICLE INFO

Article history:
Received 8 November 2020
Received in revised form 6 January 2021
Accepted 11 January 2021
Available online 4 February 2021

Editor: Henner Hollert

Keywords:
Neonicotinoids
Honeybees
Degradation
Synergy effect
Mass spectrometry imaging

ABSTRACT

Honeybees are essential for the pollination of a wide variety of crops and flowering plants, whereas they are confronting decline around the world due to the overuse of pesticides, especially neonicotinoids. The mechanism behind the negative impacts of neonicotinoids on honeybees has attracted considerable interest, yet it remains unknown due to the limited insights into the spatiotemporal distribution of pesticides in honeybees. Herein, we demonstrated the use of matrix-assisted laser desorption/ionization mass spectrometry imaging (MALDI-MSI) for the spatiotemporal visualization of neonicotinoids, such as N-nitroguanidine (dinotefuran) and N-cyanoamidine (acetamiprid) compounds, administered by oral application or direct contact, in the whole-body section of honeybees. The MSI results revealed that both dinotefuran and acetamiprid can quickly penetrate various biological barriers and distribute within the whole-body section of honeybees, but acetamiprid can be degraded much faster than dinotefuran. The degradation rate of acetamiprid is significantly decreased when piperonyl butoxide (PBO) is applied, whereas that of dinotefuran remains almost unchanged. These two factors might contribute to the fact that dinotefuran affords a higher toxicity to honeybees than acetamiprid. Moreover, the toxicity and degradation rate of acetamiprid can be affected by co-application with tebuconazole. Taken together, the results presented here indicate that the discrepant toxicity between dinotefuran and acetamiprid does not lie in the difference in their penetration of various biological barriers of honeybees, but in the

* Corresponding authors.
E-mail addresses: zbyin@agrogene.ac.cn (Z. Yin), wuxz@scau.edu.cn (X. Wu), hhxu@scau.edu.cn (H. Xu).
[1] Yue Zhang and Dong Chen contributed equally to this work.

https://doi.org/10.1016/j.scitotenv.2021.145170

degradation rate of neonicotinoid pesticides within honeybee tissues. Moreover, new perspectives are given to better understand the causes of the current decline in honeybee populations posed by insecticides, providing guidelines for the precise use of conventional agrochemicals and the rational design of novel pesticide candidates.

1. Introduction

Accounting for 80% of the insect pollinators worldwide, honeybees are of particular economic and ecological importance, as they sustain plant production of global plants around the globe and support economic values (Gill et al., 2012; Manjon et al., 2018; Wang et al., 2020a). As the most efficacious floral visitors among the existing pollinators, they play a significant role in plant biodiversity through pollinating wild plants. Honeybees also produce honey and royal jelly, which are extensively used in medicine, food and cosmetics, providing numerous benefits to humans (Decourtye et al., 2013; Potts et al., 2016). Nonetheless, recent studies have implicated a dramatic decrease in honeybee populations as exposure to pesticides, and a great quantity of colonies have exhibited generally weakening and unprecedented disappearance, which is known as colony collapse disorder (CCD) (Chen et al., 2018; Tosi et al., 2018). Additionally, the potential threat of honeybee decline has induced serious environmental concerns worldwide, and numerous interacting factors have been investigated to uncover the reasons behind the global decline of honeybees, such as pathogens, parasites, natural habitat degradation, nutritional stress and pesticide poisoning (Decourtye et al., 2013; Heard et al., 2017; Rortais et al., 2017). Although the causes of current declines in honeybee populations remain unknown, pesticide application has been proven to be closely associated with changes in honeybee behaviors and reduced colony queen production (Tao et al., 2019; Whitehorn et al., 2012). To protect plants from diseases and insect pests, virtually all agricultural products are exposed to agricultural pesticides, resulting in honeybees are inevitably exposed to numerous pesticides when foraging (Cheng et al., 2017; Goulson et al., 2015; Guglielmi et al., 2012). Additionally, herbicides may reduce the abundance and biodiversity of flowering plants and therefore also have a negative effect on honeybees (Prado et al., 2019). Despite the current decline in honeybee populations is likely caused by many factors, it comes to a general consensus that neonicotinoid pesticides are one of the main reasons for this severe declines.

Neonicotinoids, acting as agonists of the nicotinic acetylcholine receptor (nAChR), exhibit a broad insecticidal spectrum and show excellent bioactivity against insects that can be resistant to the majority of insecticides (Mitchell et al., 2017; Wintermantel et al., 2020). Thus, neonicotinoids have been widely used and occupy approximately 25% of the global agrochemical market, with annual sales up to $1.5 billion (Renaud et al., 2018). However, concern about their use has grown due to the negative impacts on honeybee health, such as causing abnormal foraging activity and damaging navigation sense, even at low doses (Li et al., 2013; Tao et al., 2019). More specifically, neonicotinoids can impair olfactory learning and memory in honeybees, which are necessary for making honey and propagating pollen, and this impairment can eventually lead to colony failure (Decourtye et al., 2003). Even worse, honeybees exposed to neonicotinoids are more sensitive to pathogens and parasites, resulting in the collapse of the colony (Prado et al., 2019). Recently, Wintermantel et al. has reported that neonicotinoids widespreadly contaminate oilseed rape nectar that causes the death of foragers and colony weakening, despite EU-wide restrictions on the application of clothianidin, imidacloprid and thiamethoxam in crops that attract honeybees (Wintermantel et al., 2020). For this reason, many studies have explored the potential mechanisms of the distinct toxicity of neonicotinoids to honeybees, especially for N-nitroguanidine compounds including dinotefuran and thiamethoxam, which are more toxic to honeybees than N-cyanoamidine compounds (e.g., acetamiprid and thiacloprid) regardless of their affinity for the receptor (Iwasa et al., 2004). However, the distribution of neonicotinoid pesticides in honeybees through direct contact or oral contact is still poorly understood. Therefore, insights into the spatiotemporal distribution of pesticides within honeybee tissues are key to deciphering the mechanisms behind their distinct toxicity.

Liquid or gas chromatography combined with mass spectrometry (LC/GC–MS) techniques has been widely used for pesticide detection, but spatiotemporal information is missing and sample preparation is time-consuming (Manjon et al., 2018). To this end, many optical imaging techniques, including fluorescence spectroscopy and isotope-labeling imaging, have been developed to monitor the distribution of pesticides within tissues. However, fluorescent tags normally disturb their original distribution and it is hard to distinguish between parent molecules and their metabolites (Catae et al., 2019). Benefiting from the unique features of visualized, label-free, and nonspecific detection, mass spectrometry imaging (MSI) has become particularly attractive for gaining the spatiotemporal distribution information of endogenous compounds within tissues and single cells (Cheng et al., 2020; Wang et al., 2020c; Yin et al., 2019). Among these methods, laser ionization mass spectrometry (LI-MS) has been applied to simultaneously detect all metal and nonmetal elements as well as the map of polymetallic nodules (Huang et al., 2011; Zhang et al., 2013). Secondary ion mass spectrometry (SIMS) has been successfully applied to detect the spatial distribution of drugs and lipids in drosophila brains (Phan et al., 2015). Desorption electrospray ionization mass spectrometry (DESI-MS) has been applied to direct and rapid detection of chloramphenicol in honey samples (Huang et al., 2014). Matrix-assisted laser desorption/ionization mass spectrometry (MALDI-MS) is widely used for the location of drug and lipid locations in various insect tissues, such as drosophila, mosquito, and diamondback moth (Khalil et al., 2015; Ohtsu et al., 2018; Yang et al., 2020a), and visualizing spatial differences in the accumulation of drugs in fishes and in the degradation of solid polycaprolactone diol (Davis et al., 2020; Rivas et al., 2016). In addition, Catae and Pratavieira have acquired neuropeptide distributions in honeybee brains using MALDI-MS imaging (Catae et al., 2019; Pratavieira et al., 2018). However, the specific distribution of pesticides in honeybees and the potential interactions between pesticides and honeybees still remain unknown.

Here, we exploited the potentials of the MALDI-MSI technique for the spatiotemporal visualization of two neonicotinoid pesticides with the similar affinity for nAChR, such as dinotefuran and acetamiprid, applied by oral or surface administration in honeybees. Given that piperonyl butoxide (PBO) has been widely used as an insecticide synergist (Iwasa et al., 2004), which could increase the toxicity of acetamiprid instead of dinotefuran, the effects of the cytochrome P450 inhibitors PBO on the spatiotemporal distributions of dinotefuran and acetamiprid in honeybees were also investigated. Considering honeybees are generally exposed to multiple pesticides simultaneously, we also investigated the spatial distributions of acetamiprid co-applied with tebuconazole. Overall, the results herein provide a scientific basis for clarifying the toxicity difference mechanism of the existing neonicotinoid pesticides and lay a foundation for designing new pesticides with lower toxicity to honeybees.

2. Materials and methods

2.1. Chemicals

Dinotefuran, acetamiprid, and tebuconazole were purchased from J&K Scientific Ltd. (Beijing, China). Phosphorylcholine, α-cyano-4-hydroxycinnamic acid (CHCA), and 2,5-dihydroxybenzoic acid (DHB) were purchased from Sigma Aldrich (St. Louis, MO, USA). The detailed

information was listed in Table S1. PBO, acetone, trifluoroacetate, paraformaldehyde, haematoxylin, eosin, paraffin wax, Tween 80 and sucrose were purchased from Energy Chemistry Ltd. (Shanghai, China). HPLC-grade acetonitrile and methanol were purchased from Tedia Company Inc. (Fairfield, OH, USA). Optimum cutting temperature (OCT) was purchased from Leica (Wetzlar, Germany).

2.2. Sample preparation of standards, pesticides and MALDI matrices

For MALDI analysis, the individual stock solutions of dinotefuran and acetamiprid were first dissolved in acetonitrile at a concentration of 1000 mg/L. Then the working solution was prepared by sequentially diluting with acetonitrile to the final concentration of 10–100 mg/L. For MSI analysis, the PBO adjuvant solution for toxicity assessment was dissolved in sucrose solution (50% w/v) at a concentration of 1000 mg/L. The stock solutions of dinotefuran, acetamiprid and tebuconazole for treating honeybees were first dissolved in acetone at the concentration of 10,000 mg/L. The working solution was prepared by diluting with sucrose solution (50%, w/v) to 100 mg/L and acetone to 1000 mg/L for oral and contact administration, respectively. The matrix solution of CHCA and DHB was prepared by a mixture of solvent comprising water–acetonitrile in a 50/50 (v/v) ratio with 0.1% trifluoroacetic acid, and the final concentration of 5 mg/mL was used for MALDI experiments. For MALDI analysis, the standard "dried droplet" method was employed to prepare MALDI targets (Wu et al., 2018). All the solutions were stored at −4 °C and warmed to room temperature before use.

2.3. Ingestion and contact toxicity assessment

Young adult worker honeybees with similar ages were captured from a disease-free and queen-right colony reared in the Key Laboratory of Natural Pesticide and Chemical Biology (South China Agricultural University, China) on the morning of our experiment. The honeybees were randomly transferred into test cages (size: $18 \times 18 \times 16$ cm^3) which had four holes on four sides and a removable gauze as the top side and was populated with approximately 30 individuals. The detailed experimental workflow for ingestion toxicity assays, contact toxicity assays, synergist PBO assays, and the co-applied tebuconazole assays were described in the Experimental Procedures of the Supplementary materials. Additionally, concentrations of insecticides (e.g., dinotefuran and imidacloprid) in oral and contact toxicity studies were listed in Table S2 (Supplementary materials). Three replicate cages were used for each treatment and maintained at 25 ± 1 °C and 75 ± 5% relative humidity in the dark except during observations. Mortality was assessed after 48 h since feeding. The honeybees that were unable to respond when touched with a fine hair brush were considered dead. Based on the results of the ingestion toxicity assessment, the time for a honeybee to become unable to stand when exposed to acetamiprid and dinotefuran was recorded for the knockdown bioassay. We chose acetamiprid concentrations of 100 and 200 mg/L and dinotefuran concentrations of 0.6 and 1.2 mg/L for oral application, and acetamiprid concentrations of 6.8 and 13.6 μg/bee and dinotefuran concentrations of 0.03 and 0.06 μg/bee for contact application, respectively. A total of 27 cages (30 honeybees per cage) were used in the experiments, with three replicate cages per concentration and three replicate cages as controls. The number of honeybees that could not stand by themselves was counted every hour after the treatment.

2.4. Honeybee collection for MALDI analysis

Initially, honeybees were captured for the ingestion and contact toxicity assessment. For ingestion toxicity, the tested honeybees were starved for 2 h and then the individual honeybee was fed with 0.1 μg dinotefuran or acetamiprid. For contact toxicity, the tested honeybees were anesthetized with CO_2 for 20 s and then 1 μL dinotefuran or acetamiprid was applied to the middle of the dorsal side of each individual honeybee. For synergist PBO assays, the individual honeybee was first treated with 10 μg of synergist PBO and then with dinotefuran and acetamiprid as mentioned above after PBO application for 1 h. For co-applied tebuconazole assays, the honeybees were first treated with 3 μg of tebuconazole and then with 0.1 μg acetamiprid by oral administration after 1 h of tebuconazole application. All honeybees were maintained at 25 ± 1 °C and 75 ± 5% relative humidity in the dark room (Han et al., 2018).

2.5. Mass spectrometry conditions for MALDI analysis

A reflectron time-of-flight mass spectrometer (TOFMS) was built in-house as described previously with a few modifications (Wu et al., 2020). Briefly, the ion source was equipped with a frequency-tripled (355 nm) Nd:YAG laser (Minilite II, Continuum Inc., San Jose, CA, USA) with a pulse duration of 5 ns. The irradiance laser was focused to ~30 μm by an aspheric lens (f = 79.0 mm, NA = 0.143, AR Coated: 350–700 nm, Thorlabs Inc., Newton, New Jersey, USA). The laser energy of 355 nm was measured by a pyroelectric detector (PE25-C, Ophir Optronics Ltd., Israel) at the exit of the laser beam without the neutral-density filter. More specifically, 5 μJ and 20 μJ of laser energy were adopted for MALDI analysis and tissue imaging, respectively. To improve mass spectral resolution, the energy dispersal of the ions was focused by a time-lag focusing technique and a double stage reflectron (Yin et al., 2017a; Yin et al., 2017b). A multichannel delay pulse generator (DG535, Standford Research System, Sunnyvale, CA, USA) was used for accurate timing modulation. The region of interest (ROI) for the whole body, brain, and thorax tissue slicing can be clearly monitored with a built-in colored CCD camera (JHSM500m, Shenzhen Jinghang Technology Co. Ltd., Shenzhen, China). A digital oscilloscope (WaveRunner 6100A, LeCroy, USA) with an analogue bandwidth of 1 GHz and a sampling rate of 5 G/s was used for recording the output signals. To achieve high throughput imaging analysis, a two-dimensional translation stage (OSMS20-85, Sigma Koki, Tokyo, Japan) was used in this study. For MSI analysis, a pixel size of 30 μm and 3 pulses for each pixel was adopted for each image.

2.6. Workflow for MSI analysis

For MALDI tissue imaging, honeybees generally undergo dissection, embedding, sectioning, matrix spraying, and MSI analysis as shown in Fig. 1. First, honeybees were collected after 2, 6, and 10 h since the start of experiments, and then they were immediately frozen in liquid nitrogen and stored at −80 °C until tissue slicing. Before embedding, the feet and wings of honeybees were first removed. Then the tissues were uniformly embedded with OCT for supporting the tissues (Phan et al., 2016), and finally sliced into 25 μm at −20 °C on a freezing microtome (CM1950, Leica Microsystems Inc., Wetzlar, Germany). The direction was parallel to the back of the honeybee thorax for the whole-body tissue and parallel to the forehead of the honeybee head for head slicing, as shown by the red arrow in Fig. S1, which makes it easier to acquire intact slices and the integrated spatial localization of the molecule of interest. Considering the stiff external waxy cuticle, the soft internal tissues and the irregular shapes of the honeybees, pretreatment of honeybees before sectioning is one of the crucial steps to guarantee the reliability and reproducibility of MSI results. The homogeneity of matrix molecules on tissue surfaces plays an important role in acquiring the MS images of samples (Yang and Caprioli, 2011), which was described in the Experimental Procedures (Supplementary materials). Microscopic images of CHCA deposition onto tissues indicated that matrix molecules were homogeneously distributed (Fig. S2). Given that the laser spot size was ~30 μm during MSI analysis (Fig. S3), a lateral resolution of 30 μm can be achieved for undistorted images.

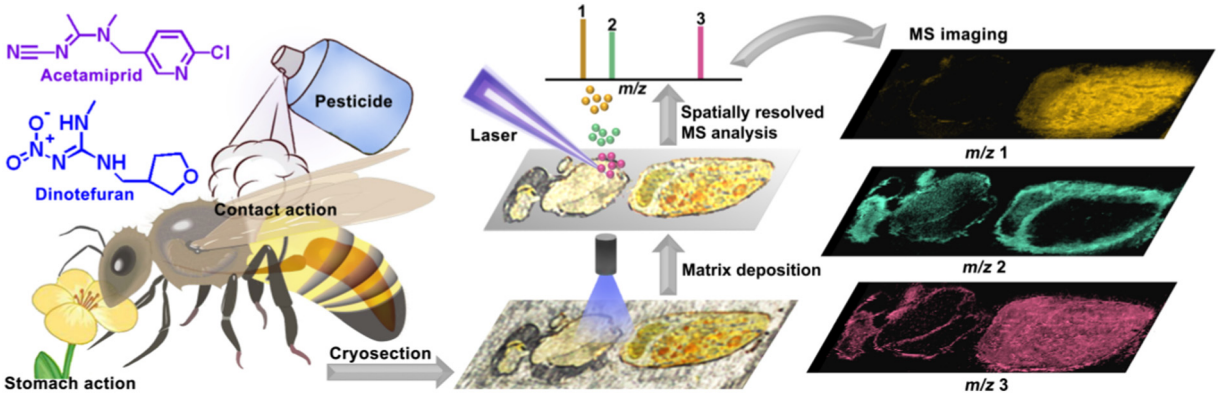

Fig. 1. Workflow of MALDI imaging of the whole-body section of honeybees.

2.7. Quantitative analysis by HPLC

For the determination of dinotefuran and acetamiprid concentrations in honeybees by HPLC (Agilent 1290B, Santa Clara, CA, USA), the same treatment protocol was adopted as that for the MSI experiments for contact toxicity assessment. Honeybees were collected after 2, 6, and 10 h since the start of the experiments, and then one honeybee was weighed (~80 mg) and immediately snap-frozen in liquid nitrogen. The frozen sample was ground and extracted with ~160 μL acetonitrile by ultrasonic treatment for 20 min. Primary secondary amine (PSA) was adopted for further cleanup. The upper layer was collected and filtered through a 0.25 μm membrane teflon filter for HPLC analysis after centrifuged at 10,000*g* for 10 min.

Samples were analyzed using an Agilent Plus-C18 column (250 mm × 4.6 mm, 5 μm) with acetonitrile/water (45/55, v/v) as the mobile phase at a flow rate of 1 mL/min. 270 nm and 245 nm were set as the appropriate detection wavelength for dinotefuran and acetamiprid, respectively. An autosampler with an injection volume of 10 μL was used. The retention time of dinotefuran and acetamiprid were approximately 4.8 and 6.5 min, respectively. For the determination of dinotefuran and acetamiprid concentrations in different parts of honeybees, honeybees were collected after 2 h since the start of the experiments. Then each honeybee was divided into three parts, such as head, thorax and abdomen, and immediately snap-frozen in liquid nitrogen. Finally, three separate samples which contained five heads, thoraxes or abdomens respectively were used for subsequent analysis. The same treatment protocol was adopted as the determination of dinotefuran and acetamiprid concentrations in honeybees by HPLC.

2.8. Data analysis

Toxicity analysis was conducted using SPSS 19.0 (Wang et al., 2020b). The MS signals obtained from a digital oscilloscope were processed by a self-compiled program written in LabVIEW2014 (National Instruments, Austin, TX, USA), providing a 4D data matrix regarding XY coordinates and the *m/z* of interest, as well as the corresponding signal intensities. Statistical analysis and mass spectra were obtained with Origin 9 software (Origin Lab, North Hampton, MA, USA). Then, molecular images of pesticides and the endogenous distribution in honeybees were constructed with Surfer 9 software (Golden Software, Inc., Golden, CO, USA) (Meng et al., 2020; Wu et al., 2020). For the MS images, each pixel was normalized to the base pixel with the highest signal intensity per image.

3. Results and discussion

3.1. Acute toxicity

Prior to demonstrating MALDI imaging of honeybee tissue samples, the toxicity of dinotefuran and acetamiprid for honeybees was investigated. The results indicated that the median lethal concentrations (LC_{50}) of dinotefuran and acetamiprid after exposure for 48 h were 0.414 and 118.382 mg/L, respectively, suggesting that dinotefuran has approximately 285-fold higher toxicity than acetamiprid (Table 1). In contrast, the median lethal doses (LD_{50}) of dinotefuran and acetamiprid after exposure for 48 h were 0.030 and 6.022 μg/bee, respectively, which is in accordance with the previous studies that reported dinotefuran affords a 200-fold higher toxicity than acetamiprid (Chen et al., 2019; Yang et al., 2020b). Moreover, toxicity data contained in Pesticide Properties Data Base (PPDB) showed the LD_{50} of dinotefuran and acetamiprid were 0.023 and 8.09 μg/bee, respectively. Also, the toxicity of dinotefuran and acetamiprid co-applied with PBO was listed in Table 1 which shows that the toxicity of acetamiprid was closely associated with PBO, but not for dinotefuran. Given PBO inhibits the metabolic enzyme systems of honeybees, such as the CYP450 superfamily, the above phenomenon can be ascribed to the fact that honeybees are able to detoxify acetamiprid to some extent. Furthermore, the toxicities of acetamiprid co-applied with fungicide tebuconazole were 14.942 mg/L for oral application and 2.051 μg/bee for contact application (Table 1), suggesting that tebuconazole, which acts as an ergosterol biosynthesis inhibitor, has a dramatic effect on increasing the toxicity of acetamiprid. To explore the time that dinotefuran and acetamiprid take to work, the median knock-down time (KT_{50}) values were evaluated at one or double of half lethal dose. The KT_{50} values of both dinotefuran and acetamiprid revealed that the smaller KT_{50} values can be obtained with higher pesticide concentration (Fig. S4).

3.2. MSI of the whole-body section of honeybees

A sagittal longitudinal whole-body tissue section of the honeybee was analyzed by MALDI-MSI to visualize the detailed distribution of pesticides and endogenous compounds across honeybees. An optical image of a sectioned whole-body tissue was displayed in Fig. 2a, indicating that the morphological structures including head, thorax, intestine, and the whole-body section can be integrally preserved. To better assign the tissue positions where the specific compounds located, an

Table 1
Acute toxicity of acetamiprid, dinotefuran and pretreatment effect of PBO and tebuconazole on honeybees by oral or topical application after 48 h.

Pesticide	Oral LC_{50} (mg/L)	95% CL	Contact LD_{50} (μg/bee)	95% CL
Acetamiprid	118.38	101.86–135.74	6.02	4.93–7.27
Dinotefuran	0.41	0.34–0.51	0.03	0.02–0.04
Acetamiprid + PBO	8.46	7.11–9.89	0.86	0.75–1.01
Dinotefuran + PBO	0.40	0.32–0.49	0.03	0.02–0.04
Acetamiprid + tebuconazole	14.94	13.08–17.13	2.05	1.57–2.58

Note: CL is the abbreviation of confidence limit.

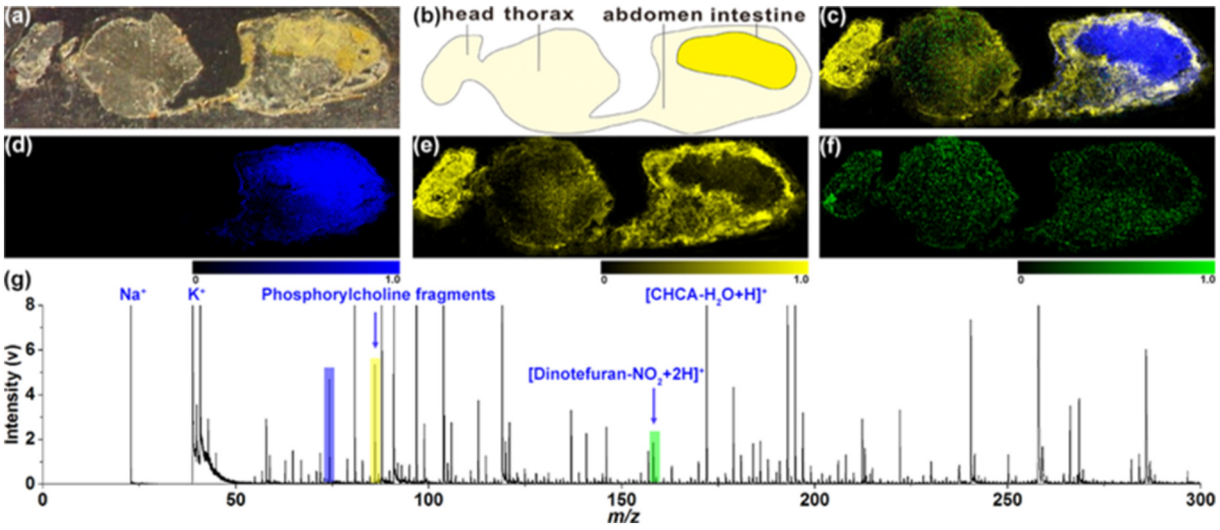

Fig. 2. MALDI images of the whole-body section of honeybees. (a) An optical image and (b) graphical representation of organ location in honeybees. (c) The merged image of three selected ions, such as two endogenous compounds at (d) *m/z* 74.3 (blue), (e) *m/z* 86.1 (yellow), and the diagnostic fragment ion of dinotefuran at (f) *m/z* 158.2 (green). (g) The typical mass spectrum of honeybees exposed to dinotefuran with 500 accumulated laser pulses. Scale bar, 1 mm.

anatomical drawing was demonstrated in Fig. 2b according to the histology of the organs. As exhibited in Fig. 2d, the endogenous compound at *m/z* 74.3 colored in blue mainly localized in the intestine and was hardly observed in other parts of the honeybee. Conversely, the phosphorylcholine fragments at *m/z* 86.1 in Fig. 2e was distributed across the whole-body section, with a higher intensity in the brain and a lower abundance in the intestine. In contrast, dinotefuran quickly penetrated the whole-body sections, yet a relatively lower concentration was observed in the intestine since 2 h of surface administration (Fig. 2f). Fig. 2c shows the integrated image with three selected ions, revealing that compounds in different tissue regions with specific morphological features could be easily distinguished. Typical mass spectrum of the whole-body section of the honeybee after exposed to dinotefuran was demonstrated in Fig. 2g. The results indicated that this MSI method could afford direct visualization of exogenous pesticides and endogenous compounds simultaneously, providing new opportunities in pesticide toxicity analysis and novel agrochemical design by precisely evaluating the dose response behavior of the individual honeybee.

3.3. Spatiotemporal distribution of dinotefuran and acetamiprid in whole-body sections of honeybees by oral administration

Honeybees are chronically exposed to neonicotinoids because flowers they forge may be contaminated with neonicotinoids (Sanchez-Bayo, 2014). Recently, some studies revealed that honeybees preferred to collect nectar containing varieties of neonicotinoids (Kessler et al., 2016). Because of the systemic distribution property in plants, neonicotinoid pesticides which could be used by spray, soil addition, or seed dressing have been detected in nectar and pollen, causing the potential contact and oral exposure of honeybees in the residue of neonicotinoids (Sanchez-Bayo, 2014). To evaluate the spatial distributions of dinotefuran and acetamiprid after oral administration, the MS images of acetamiprid and dinotefuran in honeybees were investigated. It was observed that both acetamiprid and dinotefuran can quickly penetrate various biological barriers and distribute within the whole-body sections after 2 h since oral administration and are meanwhile particularly enriched in the intestine (Fig. 3a, g). Taken together, these results verified that low KT_{50} values can be ascribed to the fact that both dinotefuran and acetamiprid can quickly penetrate through the head and expose to the targeted nAChR in the nervous system of insects. After 6 h since oral administration, the dinotefuran can uniformly distribute throughout the whole body of honeybees (Fig. 3h), whereas the content was decreased approximately to 50% for acetamiprid (Fig. 3b). The content of acetamiprid decreased until 10 h since oral administration (Fig. 3c), indicating that the lower toxicity of acetamiprid is due to its rapid degradation rate. In sharp contrast, only slow decrease of dinotefuran was observed within the same time. The above-mentioned results implied that honeybees exhibited stronger capacity to metabolize acetamiprid than dinotefuran, and thus acetamiprid is safer to honeybees than dinotefuran due to this fast metabolism. Given that both dinotefuran and acetamiprid show similar affinity for nAChR (Manjon et al., 2018), the selective toxicity between dinotefuran and acetamiprid lies in their metabolic differences rather than distinct penetration rate in various biological barriers (e.g., blood-brain barrier, and intestinal barrier) of honeybees.

Although previous researches have suggested that metabolic differences of honeybees for these two pesticides is due to their sensitivity to the CYP450 superfamily (Iwasa et al., 2004; Manjon et al., 2018), the effects of CYP450 superfamily on the degradation of these two pesticides in honeybees remain unknown. As listed in Table 1, the introduction of PBO results in a 14-fold higher toxicity of acetamiprid than that of dinotefuran. To further elucidate the influence of the CYP450 superfamily on the degradation of these two pesticides, the spatiotemporal visualizations of dinotefuran and acetamiprid with PBO as adjuvant added by oral administration were further investigated (Fig. 3). The results revealed that the spatiotemporal distribution of dinotefuran in the whole-body section of honeybees was nearly unchanged, whether PBO was added or not. However, the addition of 10 μg PBO resulted in the accumulation of acetamiprid in the intestine compared to those without PBO treatment (Fig. 3d–f). Of particular interest, given that PBO inhibited the CYP450 superfamily of honeybees which was richer in the intestine than in other parts, it was rational that acetamiprid was mainly enriched in the intestine, further supporting that the inhibition of enzymes reduces the degradation rate of acetamiprid. Altogether, the CYP450 superfamily can contribute to the metabolism of acetamiprid rather than dinotefuran for honeybees, which is in accordance with the earlier findings (Manjon et al., 2018; Wang et al., 2019). Our results demonstrated that the molecular basis of the different sensitivity of honeybees to dinotefuran and acetamiprid lies in their different metabolic rate rather than receptor affinities and biological barrier penetration of honeybees. Thus, this label-free MSI strategy

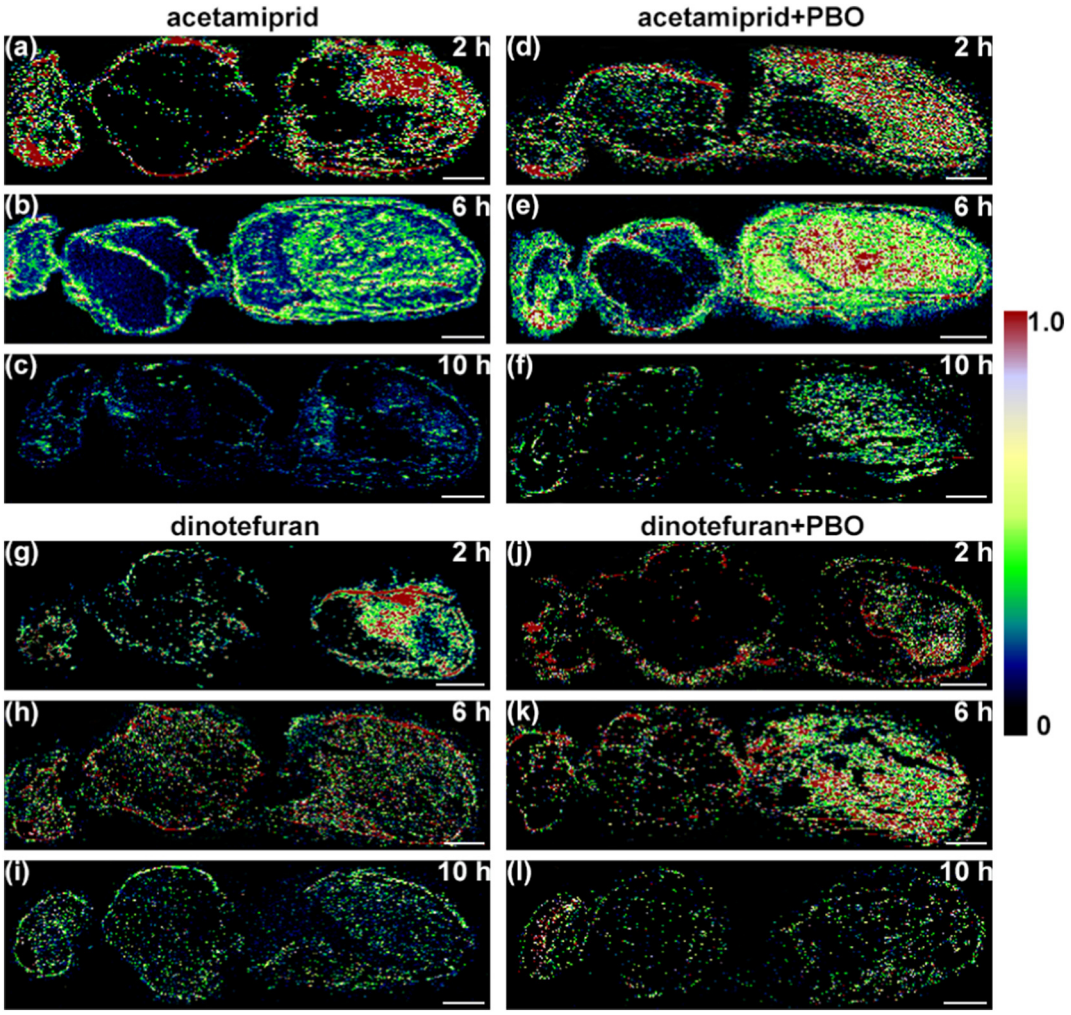

Fig. 3. MSI Analysis of acetamiprid and dinotefuran in honeybees after different oral administration times. MS images of the acetamiprid at *m/z* 223.1 after (a) 2 h, (b) 6 h, (c) 10 h and acetamiprid pretreatment with PBO after (d) 2 h, (e) 6 h, (f) 10 h application. MS images of the dinotefuran at *m/z* 158.2 after (g) 2 h, (h) 6 h, (i) 10 h and dinotefuran pretreatment with PBO after (j) 2 h, (k) 6 h, (l) 10 h application. Scale bar, 1 mm.

affords great potential in the visualization of pesticides in honeybees, uncovering the selective toxicity mechanism between dinotefuran and acetamiprid, and providing detailed guidelines for the scientific use of agrochemicals to avoid the global declines of honeybees.

3.4. The spatiotemporal distribution of dinotefuran and acetamiprid in whole-body sections of honeybees by contact administration

To evaluate the spatial distributions of acetamiprid and dinotefuran after contact administration, the MS images of dinotefuran and acetamiprid in honeybees were further investigated (Fig. 4), which indicated that both acetamiprid and dinotefuran were able to penetrate the body walls and rapidly distribute in the different compartments of honeybees after 2 h of application (Fig. 4a, g). It can be inferred that hairs on the back of the honeybee's thorax perhaps could facilitate the penetration of these chemicals into the thorax of honeybees (Fig. S5). On closer inspection, the contents of acetamiprid and dinotefuran distribution over the head were much higher through contact administration than oral administration, which might be ascribed to the fact that the application site for contact administration, the thorax, is close to the brain and ganglia. As shown in Figs. 3a and 4a, acetamiprid uniformly distributed within the whole body by contact administration than by oral administration. Moreover, acetamiprid was not particularly located in the intestine after 2 h since contact administration compared with oral administration. A detailed look at Figs. 3g and 4g revealed that similar tendency can be acquired that dinotefuran can rapidly be enriched in the intestine after 2 h since oral administration. Therefore, ingestion of these pesticides which act on the intestines of honeybees should be prevented to reduce the resultant toxicity. Additionally, their degradation rate was consistent with that by oral administration (Fig. 4a–f), further testifying that the selective toxicity between dinotefuran and acetamiprid by contact administration does not lie in their different penetration in various biological barriers. Moreover, given the small size of the insects and the large relative surface area, the body surface tends to be the important barrier for insecticides, which could help to protect honeybees from exposure to highly toxic neonicotinoids by both contact and oral administration.

To further elucidate the effect of PBO on honeybees by surface administration, MSI analysis of honeybee sections after surface administration was also conducted as shown in Fig. 4. The results disclosed that the toxicity of acetamiprid can be affected by PBO, whereas the toxicity of dinotefuran was hardly influenced. Consequently, it was further verified that the lethality evaluation of neonicotinoids to honeybees was strongly associated with the degradation rate of pesticides and the PBO which inhibits the activity of the CYP450 superfamily that plays an important role in the detoxification of acetamiprid. Of particular interest, PBO that lowers the degradation rate of pesticides in honeybees by inhibiting detoxification enzyme activities should be used with caution. Specifically, acetamiprid can be used at the flowering stage, but cannot be used with PBO for control resistance pests, while dinotefuran

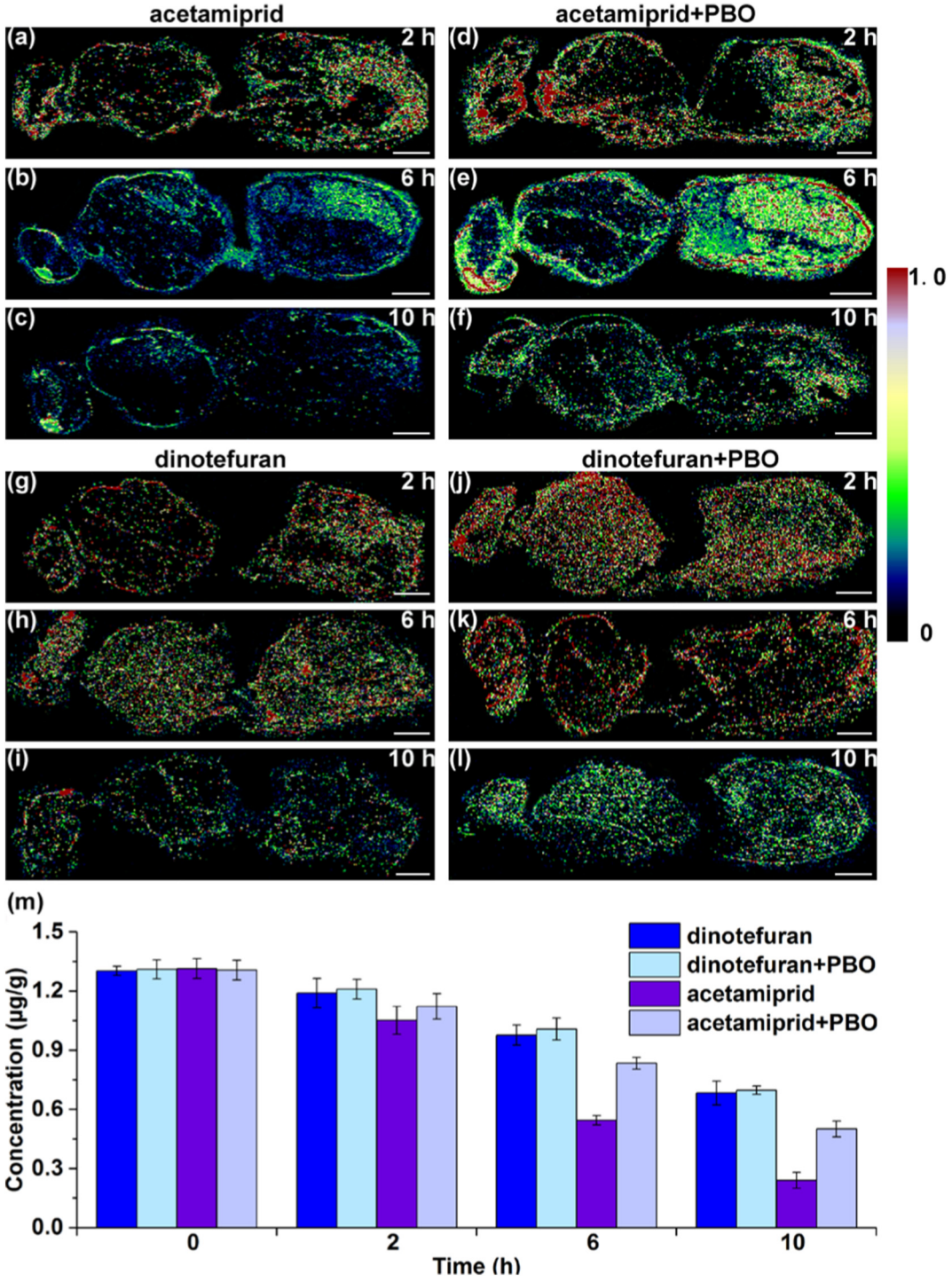

Fig. 4. MSI and HPLC analysis of acetamiprid and dinotefuran in honeybees after different surface administration times. MS images of acetamiprid after (a) 2 h, (b) 6 h, (c) 10 h application and acetamiprid pretreated with PBO after (d) 2 h, (e) 6 h, (f) 10 h application. MS images of dinotefuran after (g) 2 h, (h) 6 h, (i) 10 h application and dinotefuran pretreated with PBO after (j) 2 h, (k) 6 h, (l) 10 h. (m) Concentration of acetamiprid and dinotefuran residues in honeybees using HPLC. Scale bar, 1 mm for (a–l).

can only be used for crops not in bloom, which provides the basis for the safe and reasonable application of neonicotinoid pesticides.

3.5. Quantitative analysis by HPLC and fluorescence image of dinotefuran and acetamiprid in honeybees by contact administration

The quantitative analysis of acetamiprid and dinotefuran by homogenates of the whole honeybee was performed to estimate absolute concentrations of each pesticide in honeybees after surface administration. The pesticide concentration profiles as a function of time were shown in Fig. 4m, indicating that acetamiprid had lower concentrations in honeybee homogenates than dinotefuran after 2 h since surface administration, and the concentration of acetamiprid decreased faster than that of dinotefuran. A detailed look at Fig. 4m also revealed that the dissipation rate of acetamiprid was significantly decreased with the introduction of PBO, but that of dinotefuran presented little change, which coincided with the above MSI results, suggesting that PBO had a negative effect on acetamiprid degradation. Distribution has a fundamental

significance in determining the efficacy or toxicological properties of the pesticides. However, insights into the physiological functions of pesticides in terms of absorption, distribution, and kinetics can be hindered by stochastic average values from bulk measurements. Hence, this label-free MALDI-MSI analysis could afford in-depth localization of exogenous pesticides and endogenous compounds in a single experiment, which gives deeper insights into the toxicity of pesticides to honeybees.

3.6. Histopathology of honeybee midgut and thorax tissues after chronic toxicity

The chronic toxicity of neonicotinoids to honeybees is self-evident since high residue levels of neonicotinoids in pollen have been frequently detected (David et al., 2016; Moreno-Gonzalez et al., 2020). Numerous studies have reported that chronic toxicity of sublethal neonicotinoid doses to honeybees can damage the neurophysiological system, influence the growth of the honeybee larvae (Tavares et al., 2019), impair foraging and olfactory learning performance of worker honeybees (Shi et al., 2020), and even reduce the fecundity of honeybee queens (Sandrock et al., 2014). However, little is known about the effects of neonicotinoids on honeybee tissues after chronic exposure. In honeybees, most digestion and absorption of nutrients and chemicals occurs in the midgut, and whole-body MS images of honeybees indicated that both acetamiprid and dinotefuran could reach the midgut and thorax tissues. Therefore, the toxicity effects of acetamiprid and dinotefuran exposed to LC_{50} and LD_{50} for 2 days on the histological and cellular structure of the midgut and thorax were investigated, providing an insight into how neonicotinoids may potentially have toxicity effects on the honeybee's midgut and thorax. And our results showed that no significant morphological alterations appeared in the thorax tissues which retain morphological characteristics similar to those found in the control group whether the honeybee had acetamiprid or dinotefuran applied (Fig. 5f–j). However, both acetamiprid and dinotefuran increased the thicknesses of epithelial cells compared with that of controls, which caused the vacuolated cytoplasm in enterocytes and led to the nuclear swelling (Fig. 5a–e). Compared with orally applied dinotefuran (Fig. 5c), the adverse effects of acetamiprid were less severe (Fig. 5d). Moreover, intoxication with a sublethal dose of thiamethoxam can cause impairment in the midgut of honeybees, and increase cell elimination and apocrine secretion (Oliveira et al., 2014). Additionally, chronic expose to agrochemicals induced an increase in the chromatinic compacting level in most of the nuclei and led to the irregular nuclei (Cruz et al., 2010). Our current results indicated that the digestive and regenerative cells of the midgut after exposure to pesticides showed morphological and histochemical alterations, thus, understanding the chronic toxicity of pesticides with sublethal dosages is central to deciphering the interaction mechanism between honeybees and pesticides.

3.7. The effect of co-application with tebuconazole on spatiotemporal distribution of acetamiprid in whole-body sections of honeybees by oral administration

Several studies have reported that honeybees are chronically exposed to various pesticides instead of an individual pesticide in the natural environment (Main et al., 2020). These honeybees gathered pollen for 4 days until they were collected in the nests, and they visited a broad range of plant flowers (David et al., 2016). However, mixtures of insecticides and fungicides are frequently detected simultaneously in pollen samples of plants that need pesticides to control a wide variety of pests, diseases, weeds (Main et al., 2020). As an ergosterol-biosynthesis CYP450 inhibitor fungicide, tebuconazole has been proven to strongly synergize the toxicity of N-cyanoamidine compounds against honeybees (Iwasa et al., 2004). To this end, MSI analysis was used to clarify the synergistic effect of co-application with tebuconazole. As shown in Fig. S6, the content of acetamiprid distribution in the whole-body section of honeybees was much higher for the samples co-applied with tebuconazole than those merely treated with acetamiprid after the same application times. It can be speculated that the degradation rate of acetamiprid was significantly decreased due to the existence of tebuconazole. Recently, Wang et al. have demonstrated that nearly half of pesticides used in combination with acetamiprid had synergistic effects on honeybees (Wang et al., 2020d). Despite honeybees can detoxify a range of pesticides, exposure to these chemicals may still lead to metabolic stress and increase their susceptibility to diseases and pathogens. Therefore, it is vital for the protection of honeybees to avoid simultaneous application of pesticides that play a synergistic role until safety intervals. These findings provide novel insights into the applications of pesticides with synergistic effects to honeybees, and lay a solid foundation for the development of pesticides combinations that are less likely to have synergistic toxicity to honeybees.

3.8. MALDI images of acetamiprid and some endogenous compounds in head and thorax of honeybees

Localization and quantification of pesticides that act on the nervous system in the brain is a key indicator of efficacy in pesticide discovery and mechanistic explanation. Previous research has revealed that neonicotinoids showed agonistic affinity with nAChR which was

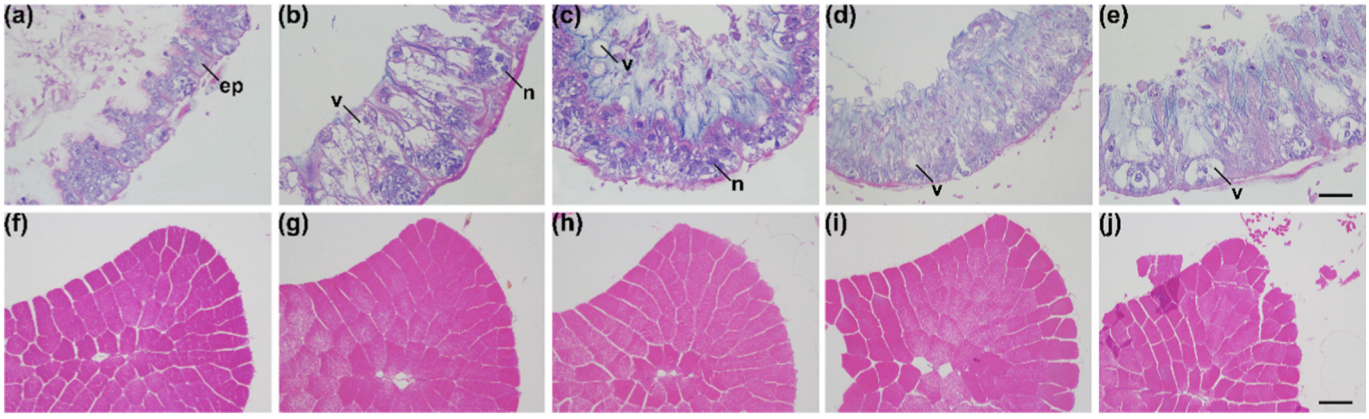

Fig. 5. Light micrographs of the midgut of honeybees. The honeybee midgut (a) without any pretreatment, with (b) LC_{50} oral exposure and (c) LD_{50} contact exposure of acetamiprid, as well as (d) LC_{50} oral exposure and (e) LD_{50} contact exposure of dinotefuran for 2 days. The honeybee thorax (f) without any pretreatment, with (g) LC_{50} oral exposure (h) LD_{50} contact exposure of acetamiprid, as well as (i) LC_{50} oral exposure and (j) LD_{50} contact exposure of dinotefuran for 2 days. (ep: epithelium, v: vacuolated, n: nuclear). Scale bar, 50 μm for (e), 200 μm for (j).

enriched in the central nervous system in the brain (Johnson, 2015). Spatiotemporal visualization of pesticides in the honeybee brain is of great importance to uncover the toxic mechanism of neonicotinoids to honeybees. To this end, MSI of acetamiprid and some endogenous compounds in the head was achieved after 2 h of oral administration (Fig. S7). The results indicated that the phosphorylcholine fragment at *m/z* 86.1 was nearly distributed through the head section except for honeybee eyes (Fig. S7e), whereas acetamiprid easily penetrated the blood-brain barrier, quickly reached the brain (Fig. S7c), and then widely located throughout the mushroom body (MB), which regulates the olfactory learning and memory functions (Wustenberg et al., 2004). Thus, the effect of neonicotinoids on the dramatic decrease in honeybee populations can be ascribed to the fact that they impair functions of the mushroom body, which is consistent with the results that acetamiprid locates in the mushroom body and acts as agonists of nAChRs in the central nervous system. As normal olfactory learning and memory functions are essential for honeybees to make honey and propagate pollen (Decourtye et al., 2003; Palmer et al., 2013), neonicotinoid exposures can cause honeybees difficulty in foraging, feeding and spreading pollen, and even lead to colony failure. MSI results of acetamiprid and some endogenous compounds in the thorax after 2 h of oral administration indicate that most endogenous compounds and acetamiprid distributed throughout the muscle tissue (Fig. S7g–l). Additionally, the quantitative mass balance of acetamiprid and dinotefuran in three regions (head, thorax and abdomen) at a given time after exposure were also obtained (Fig. S8), which revealed that both neonicotinoid pesticides were able to penetrate the body walls and rapidly distribute in the different compartments of honeybees after 2 h since application, and is consistent with MSI results.

4. Conclusion

In summary, the merit of the MALDI-MSI method for the spatiotemporal visualization of neonicotinoid agrochemicals, and their co-application with other pesticides in the whole-body sections of honeybees has been demonstrated. The results herein showed that both dinotefuran and acetamiprid quickly penetrate various biological barriers and are distributed within whole-body sections by both oral and surface administration. However, acetamiprid undergoes faster degradation than dinotefuran, supporting the conclusion that dinotefuran has a higher toxicity to honeybees than acetamiprid. Additionally, we demonstrated that the degradation rate of acetamiprid can be significantly decreased when PBO or tebuconazole was co-applied, which indicated that PBO or tebuconazole could inhibit P450 enzyme activity and slow down the detoxification of honeybees. More importantly, the selective toxicity between dinotefuran and acetamiprid does not lie in the difference in their ability to penetrate various biological barriers of honeybees (e.g., body wall barrier, intestinal barrier, and blood-brain barrier), but in their distinct degradation rates. The ability to visualize the exogenous agrochemicals and endogenous compounds in honeybee tissues with this MSI approach further provides new clues for understanding the toxic mechanism to honeybees. It might provide guidelines for the rational use of insecticides to avoid the continuation of current declines in honeybee populations.

CRediT authorship contribution statement

Yue Zhang: Conceptualization, Methodology, Performing the experiments, Writing - original draft. **Dong Chen:** Investigation, Performing the experiments, Data analysis. **Mingyi Du:** Investigation, Validation. **Lianlian Ma:** Data collection. **Ping Li:** Formal analysis. **Run Qin:** Application of statistical. **Jiaru Yang:** Provision of study materials. **Zhibin Yin:** Investigation, Supervision, Writing - review & editing, Commentary. **Xinzhou Wu:** Investigation, Supervision, Writing - review & editing, Project administration, Funding acquisition. **Hanhong Xu:** Investigation, Supervision, Project administration, Funding acquisition.

Declaration of competing interest

The authors declare that they have no known competing financial interests or personal relationships that could have appeared to influence the work reported in this paper.

Acknowledgements

We are grateful to the financial support from the Characteristic Innovation Project of Guangdong Province Ordinary University (No. 2018KTSCX025) and National Natural Science Foundation of China (No. 31901911). We also acknowledge the National Key Research and Development Program of China (No. 2018YFD0200300). This work is also supported by the Natural Science Foundation of Guangdong Province (No. 2019A1515011521).

Appendix A. Supplementary data

The supplementary data regarding experimental procedures, agrochemicals used in the experiments, concentrations of acetamiprid and dinotefuran for honeybees by oral or topical application, optical images of honeybees embedded with OCT and thorax tissues, optical images of whole-body tissues of honeybees before and after spraying with CHCA, optical images of the tissue after MALDI analysis, knock-down time of acetamiprid and dinotefuran to honeybees, MS images of honeybees whole-body sections after the co-application with tebuconazole by oral administration of acetamiprid, MS images of the brain and thorax sections for honeybees, and concentrations of acetamiprid and dinotefuran residues in different parts of honeybees after 2 h can be found in Supplementary material. Supplementary data to this article can be found online at doi:https://doi.org/10.1016/j.scitotenv.2021.145170.

References

Catae, A.F., da Silva Menegasso, A.R., Pratavieira, M., Palma, M.S., Malaspina, O., Roat, T.C., 2019. MALDI-imaging analyses of honeybee brains exposed to a neonicotinoid insecticide. Pest. Manag. Sci. 75, 607-615. "doi:https://doi.org/10.1002/ps.5226".

Chen, J., Fine, J.D., Mullin, C.A., 2018. Are organosilicon surfactants safe for bees or humans? Sci. Total Environ. 612, 415-421. "doi:https://doi.org/10.1016/j.scitotenv.2017.08.175".

Chen, Z.L., Yao, X.M., Dong, F.S., Duan, H.X., Shao, X.S., Chen, X., Yang, T., Wang, G.R., Zheng, Y.Q., 2019. Ecological toxicity reduction of dinotefuran to honeybee: new perspective from an enantiomeric level. Environ. Int. 130, 104854. "doi:https://doi.org/10.1016/j.envint.2019.05.048".

Cheng, X.L., Yin, Z.B., Rong, L., Hang, W., 2020. Subcellular chemical imaging of structurally similar acridine drugs by near-field laser desorption/laser postionization mass spectrometry. Nano. Res. 13, 745-751. "doi:https://doi.org/10.1007/s12274-020-2686-z".

Cheng, Z.P., Dong, F.S., Xu, J., Liu, X.G., Wu, X.H., Chen, Z.L., Pan, X.L., Gan, J., Zheng, Y.Q., 2017. Simultaneous determination of organophosphorus pesticides in fruits and vegetables using atmospheric pressure gas chromatography quadrupole-time-of-flight mass spectrometry. Food Chem. 231, 365-373. "doi:https://doi.org/10.1016/j.foodchem.2017.03.157".

Cruz, A.S., Silva-Zacarin, E.C.M., Bueno, O.C., Malaspina, O., 2010. Morphological alterations induced by boric acid and fipronil in the midgut of worker honeybee (*Apis mellifera* L.) larvae : morphological alterations in the midgut of *A. mellifera*. Cell Biol. Toxicol. 26, 165-176. "doi:https://doi.org/10.1007/s10565-009-9126-x".

David, A., Botias, C., Abdul-Sada, A., Nicholls, E., Rotheray, E.L., Hill, E.M., Goulson, D., 2016. Widespread contamination of wildflower and bee-collected pollen with complex mixtures of neonicotinoids and fungicides commonly applied to crops. Environ. Int. 88, 169-178. "doi:https://doi.org/10.1016/j.envint.2015.12.011".

Davis, R.B., Hoang, J.A., Rizzo, S.M., Hassan, D., Potter, B.J., Tucker, K.R., 2020. Quantitation and localization of beta-blockers and SSRIs accumulation in fathead minnows by complementary mass spectrometry analyses. Sci. Total Environ. 741, 140331. "doi:https://doi.org/10.1016/j.scitotenv.2020.140331".

Decourtye, A., Lacassie, E., Pham-Delegue, M.H., 2003. Learning performances of honeybees (*Apis mellifera* L) are differentially affected by imidacloprid according to the season. Pest. Manag. Sci. 59, 269-278. "doi:https://doi.org/10.1002/ps.631".

Decourtye, A., Henry, M., Desneux, N., 2013. Environment: overhaul pesticide testing on bees. Nature 497, 188. "doi:https://doi.org/10.1038/497188a".

Gill, R.J., Ramos-Rodriguez, O., Raine, N.E., 2012. Combined pesticide exposure severely affects individual- and colony-level traits in bees. Nature 491, 105-119. "doi:https://doi.org/10.1038/nature11585".

Goulson, D., Nicholls, E., Botias, C., Rotheray, E.L., 2015. Bee declines driven by combined stress from parasites, pesticides, and lack of flowers. Science 347, 10. "doi:https://doi.org/10.1126/science.1255957".

Guglielmi, M.-A., Rocher, F., Legros, S., Bonnemain, J.-L., Chollet, J.-F., 2012. A non-destructive method for testing two components of the behaviour of soil-applied agricultural chemicals over a long period. Pest. Manag. Sci. 68, 897-905. "doi:https://doi.org/10.1002/ps.3248".

Han, W.S., Wang, Y.J., Gao, J.L., Wang, S.J., Zhao, S., Liu, J.F., Zhong, Y.H., Zhao, D.X., 2018. Acute toxicity and sublethal effects of myclobutanil on respiration, flight and detoxification enzymes in *Apis cerana* cerana. Pestic. Biochem. Phys. 147, 133-138. "doi:https://doi.org/10.1016/j.pestbp.2017.11.001".

Heard, M.S., Baas, J., Dorne, J.-L., Lahive, E., Robinson, A.G., Rortais, A., Spurgeon, D.J., Svendsen, C., Hesketh, H., 2017. Comparative toxicity of pesticides and environmental contaminants in bees: are honey bees a useful proxy for wild bee species? Sci. Total Environ. 578, 357-365. "doi:https://doi.org/10.1016/j.scitotenv.2016.10.180".

Huang, R.F., Zhang, B.C., Zou, D.X., Hang, W., He, J.A., Huang, B.L., 2011. Elemental imaging via laser ionization orthogonal time-of-flight mass spectrometry. Anal. Chem. 83, 1102-1107. "doi:https://doi.org/10.1021/ac1029693".

Huang, X.Y., Fang, X.W., Zhang, X., Dai, X.M., Guo, X.L., Chen, H.W., Luo, L.P., 2014. Direct detection of chloramphenicol in honey by neutral desorption-extractive electrospray ionization mass spectrometry. Anal. Bioanal. Chem. 406, 7705-7714. "doi:https://doi.org/10.1007/s00216-014-8176-y".

Iwasa, T., Motoyama, N., Ambrose, J.T., Roe, R.M., 2004. Mechanism for the differential toxicity of neonicotinoid insecticides in the honey bee, *Apis mellifera*. Crop Prot. 23, 371-378. "doi:https://doi.org/10.1016/j.cropro.2003.08.018".

Johnson, R.M., 2015. Honey bee toxicology. Annu. Rev. Entomol. 60, 415-434. "doi:https://doi.org/10.1146/annurev-ento-011613-162005".

Kessler, S.C., Tiedeken, E.J., Simcock, K.L., Derveau, S., Mitchell, J., Softley, S., Radcliffe, A., Stout, J.C., Wright, G.A., 2016. Bees prefer foods containing neonicotinoid pesticides. Nature 533, 1. "doi:https://doi.org/10.1038/nature17177".

Khalil, S.M., Rompp, A., Pretzel, J., Becker, K., Spengler, B., 2015. Phospholipid topography of whole-body sections of the *Anopheles stephensi* mosquito, characterized by high-resolution atmospheric-pressure scanning microprobe matrix-assisted laser desorption/ionization mass spectrometry imaging. Anal. Chem. 87, 11309-11316. "doi:https://doi.org/10.1021/acs.analchem.5b02781".

Li, J.Y., Zhang, J.B., Li, C., Wang, W., Yang, Z., Wang, H.Y., Gan, J., Ye, Q.F., Xu, X.Y., Li, Z., 2013. Stereoisomeric isolation and stereoselective fate of insecticide paichongding in flooded paddy soils. Environ. Sci. Technol. 47, 12768-12774. "doi:https://doi.org/10.1021/es401279u".

Main, A.R., Hladik, M.L., Webb, E.B., Goyne, K.W., Mengel, D., 2020. Beyond neonicotinoids - wild pollinators are exposed to a range of pesticides while foraging in agroecosystems. Sci. Total Environ. 742, 140436. "doi:https://doi.org/10.1016/j.scitotenv.2020.140436".

Manjon, C., Troczka, B.J., Zaworra, M., Beadle, K., Randall, E., Hertlein, G., Singh, K.S., Zimmer, C.T., Homem, R.A., Lueke, B., Reid, R., Kor, L., Kohler, M., Benting, J., Williamson, M.S., Davies, T.G.E., Field, L.M., Bass, C., Nauen, R., 2018. Unravelling the molecular determinants of bee sensitivity to neonicotinoid insecticides. Curr. Biol. 28, 1137-1143. "doi:https://doi.org/10.1016/j.cub.2018.02.045".

Meng, Y.F., Cheng, X.L., Wang, T.T., Hang, W., Li, X.P., Nie, W., Liu, R., Lin, Z., Hang, L., Yin, Z.B., Zhang, B.L., Yan, X.M., 2020. Micro-lensed fiber laser desorption mass spectrometry imaging reveals subcellular distribution of drugs within single cells. Angew. Chem. Int. Ed. 59, 2-10. "doi:https://doi.org/10.1002/anie.202002151".

Mitchell, E.A.D., Mulhauser, B., Mulot, M., Mutabazi, A., Glauser, G., Aebi, A., 2017. A worldwide survey of neonicotinoids in honey. Science 358, 109-111. "doi:https://doi.org/10.1126/science.aan3684".

Moreno-Gonzalez, D., Cutillas, V., Dolores Hernando, M., Alcantara-Duran, J., Garcia-Reyes, J.F., Molina-Diaz, A., 2020. Quantitative determination of pesticide residues in specific parts of bee specimens by nanoflow liquid chromatography high resolution mass spectrometry. Sci. Total Environ. 715, 137005. "doi:https://doi.org/10.1016/j.scitotenv.2020.137005".

Ohtsu, S., Yamaguchi, M., Nishiwaki, H., Fukusaki, E., Shimma, S., 2018. Development of a visualization method for imidacloprid in *Drosophila melanogaster* via imaging mass spectrometry. Anal. Sci. 34, 991-996. "doi:https://doi.org/10.2116/analsci.18SCP04".

Oliveira, R.A., Roat, T.C., Carvalho, S.M., Malaspina, O., 2014. Side-effects of thiamethoxam on the brain and midgut of the Africanized honeybee *Apis mellifera* (Hymenopptera: Apidae). Environ. Toxicol. 29, 1122-1133. "doi:https://doi.org/10.1002/tox.21842".

Palmer, M.J., Moffat, C., Saranzewa, N., Harvey, J., Wright, G.A., Connolly, C.N., 2013. Cholinergic pesticides cause mushroom body neuronal inactivation in honeybees. Nat. Commun. 4, 1634. "doi:https://doi.org/10.1038/ncomms2648".

Phan, N.T.N., Fletcher, J.S., Ewing, A.G., 2015. Lipid structural effects of oral administration of methylphenidate in *Drosophila* brain by secondary ion mass spectrometry imaging. Anal. Chem. 87, 4063-4071. "doi:https://doi.org/10.1021/acs.analchem.5b00555".

Phan, N.T.N., Mohammadi, A.S., Pour, M.D., Ewing, A.G., 2016. Laser desorption ionization mass spectrometry imaging of *Drosophila* brain using matrix sublimation versus modification with nanoparticles. Anal. Chem. 88, 1734-1741. "doi:https://doi.org/10.1021/acs.analchem.5b03942".

Potts, S.G., Imperatriz-Fonseca, V., Ngo, H.T., Aizen, M.A., Biesmeijer, J.C., Breeze, T.D., Dicks, L.V., Garibaldi, L.A., Hill, R., Settele, J., Vanbergen, A.J., 2016. Safeguarding pollinators and their values to human well-being. Nature 540, 220-229. "doi:https://doi.org/10.1038/nature20588".

Prado, A., Pioz, M., Vidau, C., Requier, F., Jury, M., Crauser, D., Brunet, J.-L., Le Conte, Y., Alaux, C., 2019. Exposure to pollen-bound pesticide mixtures induces longer-lived but less efficient honey bees. Sci. Total Environ. 650, 1250-1260. "doi:https://doi.org/10.1016/j.scitotenv.2018.09.102".

Pratavieira, M., Menegasso, A.R.D., Esteves, F.G., Sato, K.U., Malaspina, O., Palma, M.S., 2018. MALDI imaging analysis of neuropeptides in Africanized honeybee (*Apis mellifera*) brain: effect of aggressiveness. J. Proteome Res. 17, 2358-2369. "doi:https://doi.org/10.1021/acs.jproteome.8b00098".

Renaud, M., Akeju, T., Natal-da-Luz, T., Leston, S., Rosa, J., Ramos, F., Sousa, J.P., Azevedo-Pereira, H.M.V.S., 2018. Effects of the neonicotinoids acetamiprid and thiacloprid in their commercial formulations on soil fauna. Chemosphere 194, 85-93. "doi:https://doi.org/10.1016/j.chemosphere.2017.11.102".

Rivas, D., Ginebreda, A., Perez, S., Quero, C., Barcelo, D., 2016. MALDI-TOF MS Imaging evidences spatial differences in the degradation of solid polycaprolactone diol in water under aerobic and denitrifying conditions. Sci. Total Environ. 566, 27-33. "doi:https://doi.org/10.1016/j.scitotenv.2016.05.090".

Rortais, A., Arnold, G., Dorne, J.-L., More, S.J., Sperandio, G., Streissl, F., Szentes, C., Verdonck, F., 2017. Risk assessment of pesticides and other stressors in bees: principles, data gaps and perspectives from the European Food Safety Authority. Sci. Total Environ. 587, 524-537. "doi:https://doi.org/10.1016/j.scitotenv.2016.09.127".

Sanchez-Bayo, F., 2014. The trouble with neonicotinoids. Science 346, 806-807. "doi:https://doi.org/10.1126/science.1259159".

Sandrock, C., Tanadini, L.G., Pettis, J.S., Biesmeijer, J.C., Potts, S.G., Neumann, P., 2014. Sublethal neonicotinoid insecticide exposure reduces solitary bee reproductive success. Agr. Forest Entomol. 16, 119-128. "doi:https://doi.org/10.1111/afe.12041".

Shi, J.L., Yang, H.Y., Yu, L.T., Liao, C.H., Liu, Y., Jin, M.J., Yan, W.Y., Wu, X.B., 2020. Sublethal acetamiprid doses negatively affect the lifespans and foraging behaviors of honey bee (*Apis mellifera* L.) workers. Sci. Total Environ. 738, 139924-139924. "doi:https://doi.org/10.1016/j.scitotenv.2020.139924".

Tao, Y., Dong, F.S., Xu, J., Dung, P., Liu, Q.Y., Li, R.N., Liu, X.G., Wu, X.H., He, M., Zheng, Y.Q., 2019. Characteristics of neonicotinoid imidacloprid in urine following exposure of humans to orchards in China. Environ. Int. 132, 105079. "doi:https://doi.org/10.1016/j.envint.2019.105079".

Tavares, D.A., Roat, T.C., Mathias Silva-Zacarin, E.C., Ferreira Noceelli, R.C., Malaspina, O., 2019. Exposure to thiamethoxam during the larval phase affects synapsin levels in the brain of the honey bee. Ecotox. Environ. Safe. 169, 523-528. "doi:https://doi.org/10.1016/j.ecoenv.2018.11.048".

Tosi, S., Costa, C., Vesco, U., Quaglia, G., Guido, G., 2018. A 3-year survey of Italian honey bee-collected pollen reveals widespread contamination by agricultural pesticides. Sci. Total Environ. 615, 208-218. "doi:https://doi.org/10.1016/j.scitotenv.2017.09.226".

Wang, F., Yang, J.F., Wang, M.Y., Jia, C.Y., Shi, X.X., Hao, G.F., Yang, G.F., 2020a. Graph attention convolutional neural network model for chemical poisoning of honey bees? prediction. Sci. Bull. 65, 1184-1191. "doi:https://doi.org/10.1016/j.scib.2020.04.006".

Wang, J., Jia, B., Li, Y.H., Ren, B., Liang, H.L., Yan, D.Y., Xie, H.Y., Zhang, X.D., Liang, H.W., 2020b. Effects of multi-walled carbon nanotubes on the enantioselective toxicity of the chiral insecticide indoxacarb toward zebrafish (Danio rerio). J. Hazard. Mater. 397, 122724. "doi:https://doi.org/10.1016/j.jhazmat.2020.122724".

Wang, J.Q., Ohno, H., Ide, Y., Ichinose, H., Mori, T., Kawagishi, H., Hirai, H., 2019. Identification of the cytochrome P450 involved in the degradation of neonicotinoid insecticide acetamiprid in *Phanerochaete chrysosporium*. J. Hazard. Mater. 371, 494-498. "doi:https://doi.org/10.1016/j.jhazmat.2019.03.042".

Wang, T.T., Cheng, X.L., Xu, H.X., Meng, Y.F., Yin, Z.B., Li, X.P., Hang, W., 2020c. Perspective on advances in laser-based high-resolution mass spectrometry imaging. Anal. Chem. 92, 543-553. "doi:https://doi.org/10.1021/acs.analchem.9b04067".

Wang, Y.H., Zhu, Y.C., Li, W.H., 2020d. Interaction patterns and combined toxic effects of acetamiprid in combination with seven pesticides on honey bee (*Apis mellifera* L.). Ecotox. Environ. Safe. 190, 110100. "doi:https://doi.org/10.1016/j.ecoenv.2019.110100".

Whitehorn, P.R., O'Connor, S., Wackers, F.L., Goulson, D., 2012. Neonicotinoid pesticide reduces bumble bee colony growth and queen production. Science 336, 351-352. "doi:https://doi.org/10.1126/science.1215025".

Wintermantel, D., Odoux, J.-F., Decourtye, A., Henry, M., Allier, F., Bretagnolle, V., 2020. Neonicotinoid-induced mortality risk for bees foraging on oilseed rape nectar persists despite EU moratorium. Sci. Total Environ. 704, 135400. "doi:https://doi.org/10.1016/j.scitotenv.2019.135400".

Wu, X.Z., Li, W.F., Guo, P.R., Zhang, Z.X., Xu, H.H., 2018. Rapid trace detection and isomer quantitation of qesticide residues via matrix-assisted laser desorption/lonization fourier transform ion cyclotron resonance mass spectrometry. J. Agr. Food Chem. 66, 3966-3974. "doi:https://doi.org/10.1021/acs.jafc.8b00427".

Wu, X.Z., Qin, R., Wu, H.X., Yao, G.K., Zhang, Y., Li, P., Xu, Y.Z., Zhang, Z.X., Yin, Z.B., Xu, H.H., 2020. Nanoparticle-immersed paper imprinting mass spectrometry imaging reveals uptake and translocation mechanism of pesticides in plants. Nano. Res. 13, 611-620. "doi:https://doi.org/10.1007/s12274-020-2700-5".

Wustenberg, D.G., Boytcheva, M., Grunewald, B., Byrne, J.H., Menzel, R., Baxter, D.A., 2004. Current- and voltage-clamp recordings and computer simulations of kenyon cells in the honeybee. J. Neurophysiol. 92, 2589-2603. "doi:https://doi.org/10.1152/jn.01259.2003".

Yang, F.Y., Chen, J.H., Ruan, Q.Q., Saqib, H.S.A., He, W.Y., You, M.S., 2020a. Mass spectrometry imaging: an emerging technology for the analysis of metabolites in insects. Arch. Insect Biochem. 103, 11. "doi:https://doi.org/10.1002/arch.21643".

Yang, J.H., Caprioli, R.M., 2011. Matrix sublimation/recrystallization for imaging proteins by mass spectrometry at high spatial resolution. Anal. Chem. 83, 5728-5734. "doi:https://doi.org/10.1021/ac200998a".

Yang, Y., Ma, S.L., Liu, F., Wang, Q., Wang, X., Hou, C.S., Wu, Y.Y., Gao, J., Zhang, L., Liu, Y.J., Diao, Q.Y., Dai, P.L., 2020b. Acute and chronic toxicity of acetamiprid, carbaryl, cypermethrin and deltamethrin to *Apis mellifera* larvae reared in vitro. Pest. Manag. Sci. 76, 978-985. "doi:https://doi.org/10.1002/ps.5606".

Yin, Z.B., Cheng, X.L., Liu, R., Hang, W., Huang, B.L., 2017a. Depth profiling of nanometer thin layers by laser desorption and laser postionization time-of-flight mass spectrometry. J. Anal. Atom. Spectrom. 32, 1878-1884. "doi:https://doi.org/10.1039/c7ja00081b".

Yin, Z.B., Xu, Z.Y., Liu, R., Hang, W., Huang, B.L., 2017b. Microtrace analysis of rare earth element residues in femtogram quantities by laser desorption and laser postionization mass spectrometry. Anal. Chem. 89, 7455-7461. "doi:https://doi.org/10.1021/acs.analchem.7b01033".

Yin, Z.B., Cheng, X.L., Liu, R., Li, X.P., Hang, L., Hang, W., Xu, J.Y., Yan, X.M., Li, J.F., Tian, Z.Q., 2019. Chemical and topographical single-cell imaging by near-field desorption mass spectrometry. Angew. Chem. Int. Ed. 58, 4541-4546. "doi:https://doi.org/10.1002/anie.201813744".

Zhang, B.C., Zou, D.X., Huang, R.F., Liu, G.S., Gong, Z.B., Hang, W., Huang, B.L., 2013. Study on distribution of elements in deep-sea pacific polymetallic nodules via two-dimensional mapping laser ionization orthogonal time-of-flight mass spectrometry. Spectrochim. Acta. B. 85, 13-19. "doi:https://doi.org/10.1016/j.sab.2013.03.007".